Stochastic uncertainty analysis for solute transport in randomly heterogeneous media using a Karhunen-Loève-based moment equation approach

Gaisheng Liu,[1] Zhiming Lu,[2] and Dongxiao Zhang[3,4,5]

Received 22 May 2006; revised 14 March 2007; accepted 19 April 2007; published 18 July 2007.

[1] A new approach has been developed for solving solute transport problems in randomly heterogeneous media using the Karhunen-Loève-based moment equation (KLME) technique proposed by Zhang and Lu (2004). The KLME approach combines the Karhunen-Loève decomposition of the underlying random conductivity field and the perturbative and polynomial expansions of dependent variables including the hydraulic head, flow velocity, dispersion coefficient, and solute concentration. The equations obtained in this approach are sequential, and their structure is formulated in the same form as the original governing equations such that any existing simulator, such as Modular Three-Dimensional Multispecies Transport Model for Simulation of Advection, Dispersion, and Chemical Reactions of Contaminants in Groundwater Systems (MT3DMS), can be directly applied as the solver. Through a series of two-dimensional examples, the validity of the KLME approach is evaluated against the classical Monte Carlo simulations. Results indicate that under the flow and transport conditions examined in this work, the KLME approach provides an accurate representation of the mean concentration. For the concentration variance, the accuracy of the KLME approach is good when the conductivity variance is 0.5. As the conductivity variance increases up to 1.0, the mismatch on the concentration variance becomes large, although the mean concentration can still be accurately reproduced by the KLME approach. Our results also indicate that when the conductivity variance is relatively large, neglecting the effects of the cross terms between velocity fluctuations and local dispersivities, as done in some previous studies, can produce noticeable errors, and a rigorous treatment of the dispersion terms becomes more appropriate.

Citation: Liu, G., Z. Lu, and D. Zhang (2007), Stochastic uncertainty analysis for solute transport in randomly heterogeneous media using a Karhunen-Loève-based moment equation approach, *Water Resour. Res.*, *43*, W07427, doi:10.1029/2006WR005193.

1. Introduction

[2] Subsurface fluid flow and transport processes often take place in a complex geologic setting where permeability, the key medium property in controlling flow and transport behaviors, exhibits a high degree of spatial variability and cannot be accurately characterized in all the details. As a result, our model predictions of flow velocities and solute concentrations are subject to a great deal of uncertainty. To address the uncertainty issue in subsurface flow and transport modeling, stochastic approaches have been developed [*Dagan*, 1989; *Gelhar*, 1993; *Cushman*, 1997; *Zhang*, 2002; *Rubin*, 2003].

[3] The majority of stochastic transport research has emphasized on reproducing the ensemble averaged plume behaviors using effective macrodispersion coefficients [*Gelhar et al.*, 1979; *Dagan*, 1984; *Neuman and Zhang*, 1990; *Hu et al.*, 1999; *Salandin and Fiorotto*, 2000; *Darvini and Salandin*, 2006]. Although the macrodispersion approach provides a reasonable representation of the gross spatial spreading of solutes due to random heterogeneity in permeability, it does not provide an estimation of the uncertainty associated with the mean predictions (i.e., fluctuations around mean concentrations or concentration variances). Since the early 1990s, concentration variance has become a subject of great interest in various studies [*Dagan et al.*, 1992; *Neuman*, 1993; *Kapoor and Gelhar*, 1994a, 1994b; *Zhang and Neuman*, 1996; *Dagan and Fiori*, 1997; *Kapoor and Kitanidis*, 1997; *Morales-Casique et al.*, 2006a, 2006b]. It has been demonstrated that while the local-scale dispersion has a relatively insignificant impact on the mean concentration predictions as compared to the field-scale heterogeneities, it can exert a strong influence on the concentration variance.

[1] Kansas Geological Survey, University of Kansas, Lawrence, Kansas, USA.
[2] Hydrology and Geochemistry Group, Los Alamos National Laboratory, Los Alamos, New Mexico, USA.
[3] Mewbourne School of Petroleum and Geological Engineering, University of Oklahoma, Norman, Oklahoma, USA.
[4] Also at Department of Energy and Resources Engineering, College of Engineering, Peking University, Beijing, China.
[5] Now at Department of Civil and Environmental Engineering and Mork Family Department of Chemical Engineering and Material Sciences, University of Southern California, Los Angeles, California, USA.

0043-1397/07/2006WR005193$09.00

[4] Stochastic approaches can be generally sorted into two different frameworks, namely, Monte Carlo (MC) simulations and the moment equation (ME) approaches. Since the MC method is a brute force approach, it is computationally demanding for large-scale problems and typically serves only a benchmark role for evaluating the accuracy of other approaches [*Graham and McLaughlin*, 1989; *Hassan et al.*, 1998]. In the ME approaches the statistical moment equations are directly derived for model predictions using the perturbation technique [*Neuman*, 1993; *Kapoor and Gelhar*, 1994a, 1994b; *Zhang and Neuman*, 1995, 1996; *Kapoor and Kitanidis*, 1997; *Hu et al.*, 1999; *Salandin and Fiorotto*, 2000; *Morales-Casique et al.*, 2006a, 2006b]. Through both theoretical investigations and field data analysis, *Kapoor and Gelhar* [1994a, 1994b] demonstrated the important role of local dispersion in attenuating the concentration variance over time. To mitigate the closure problems caused by neglecting the triplet term in the macrodispersive flux in the Eulerian approach, *Hu et al.* [1999] expanded the concentration as an infinite series instead of the mean and perturbation decomposition. The mean concentrations and spatial moments were solved in the Fourier-Laplace space up to different expansion orders in flow and transport, respectively. *Salandin and Fiorotto* [2000] depicted an analytical procedure that allows estimation of the global dispersion tensor by taking into account both the pore-scale dispersion and local-scale velocity fluctuations. *Morales-Casique et al.* [2006a, 2006b] presented the first and second MEs for advective-dispersive transport and proposed a higher-order iterative closure scheme for a special case of steady state flow with respect to the first order in conductivity variance.

[5] Compared to the MC simulations, the perturbative moment solutions of stochastic flow and transport problems are formally limited to mild medium variability although data conditioning can certainly increase the effective range to some extent. More recently, *Neuman* [2006] suggested combining fractal and variational multiscale decompositions in order to extend the applicability of perturbative ME approaches in composite media where the heterogeneity can be arbitrarily large. In general, analytical solutions of the moment equations can be obtained with the aid of Green's function for some limiting cases under simplified conditions. Numerical ME approaches are conceivable, but the computational effort increases rapidly with the size of the problem, thus limiting its applicability to large-scale problems.

[6] In recent years a new class of stochastic approaches have been developed that rely on the Karhunen-Loève (KL) decomposition of the underlying random fields [*Ghanem and Spanos*, 1991; *Ghanem and Dham*, 1998; *Zhang and Lu*, 2004]. Unlike the conventional ME counterparts, the KL-based approaches do not require solving the covariance and cross-covariance matrices directly and thus become more efficient computationally. *Ghanem and Dham* [1998] combined the KL decomposition of random permeability field and the orthogonal polynomial chaos expansions of other stochastic dependent variables and applied the KL/polynomial chaos method to a two-dimensional (2-D) multiphase flow problem. *Zhang and Lu* [2004] proposed to integrate the KL decomposition with perturbative and polynomial expansions of stochastic dependent variables, and the resulting methodology was referred to as the Karhunen-Loève-based moment equation (KLME). In contrast to the KL/polynomial chaos method where equations of different orders are interactively coupled, the equations in the KLME approach are recursive and can be solved sequentially from low to high orders. The KLME approach has been applied to different types of problems including conditional simulations, saturated-unsaturated, steady state two-phase and unconfined flow [*Lu and Zhang*, 2004; *Yang et al.*, 2004; *Chen et al.*, 2005; *Liu et al.*, 2006].

[7] Motivated by the recent success in its flow applications, we apply the KLME technique to solve the stochastic solute transport problems in this work. Both the mean concentration and concentration variance are calculated. Because of its importance, the local dispersion is included and implemented in a rigorous manner. Some previous studies [*Kapoor and Gelhar*, 1994a, 1994b; *Zhang and Neuman*, 1996; *Hu et al.*, 1999; *Morales-Casique et al.*, 2006a, 2006b] treated local dispersion as either a given constant or a linear function of mean flow velocities. Consistent with *Salandin and Fiorotto* [2000], here we shall demonstrate that this simple approximation has somehow underestimated the heterogeneity effects on dispersion and can produce inappropriate results under certain circumstances.

[8] The remainder of the paper is organized as follows. We begin with a description of the mathematical model that includes advection, dispersion, and external sinks/sources. Next, we present the theoretical derivations of stochastic transport formulations using the KLME approach and describe the solution procedure. Finally, we evaluate the validity of the KLME approach with a series of 2-D examples by comparing to the results from MC simulations.

2. Methodology

2.1. Mathematic Model

[9] The transport of a conservative solute in 3-D groundwater flow under the advection, dispersion and external sinks/sources is given as

$$\frac{\partial C(\boldsymbol{x},t)}{\partial t} = \nabla \cdot (D(\boldsymbol{x},t)\nabla C(\boldsymbol{x},t)) - \nabla \cdot (v(\boldsymbol{x},t)C(\boldsymbol{x},t)) + q_s C_s, \tag{1a}$$

subject to the following initial and boundary conditions:

$$C(\boldsymbol{x},0) = C_0(\boldsymbol{x}), \qquad \boldsymbol{x} \in \Omega, \tag{1b}$$

$$C(\boldsymbol{x},t) = C_D(\boldsymbol{x},t), \qquad \boldsymbol{x} \in \Gamma_D, \tag{1c}$$

$$D(\boldsymbol{x},t)\nabla C(\boldsymbol{x},t) \cdot \boldsymbol{n}(\boldsymbol{x}) = -F(\boldsymbol{x},t), \qquad \boldsymbol{x} \in \Gamma_N, \tag{1d}$$

where C is the solute concentration; D is the hydrodynamic dispersion tensor; v is the pore water velocity vector $(v_x(\boldsymbol{x}, t), v_y(\boldsymbol{x}, t), \boldsymbol{v}_z(\boldsymbol{x}, t))^T$ (where superscript T indicates transpose); q_s and C_s are the flow rate and solute concentration in the sinks/sources; $\boldsymbol{x}$ is the vector of spatial Cartesian coordinate $(x, y, z)^T$; t is time; C_0 is the initial concentration in the transport domain Ω; $C_D(\boldsymbol{x}, t)$ is the specified concentration

on the Dirichlet boundary segments Γ_D; $F(\boldsymbol{x}, t)$ is the dispersive flux across the Neumann boundary segments Γ_N; and $\boldsymbol{n}(\boldsymbol{x})$ is an outward unit vector normal to the boundary $\Gamma_D \cup \Gamma_N$. For simplicity, the spatial and temporal indices $\boldsymbol{x}$ and t are omitted in the remainder of paper.

[10] The hydrodynamic dispersion tensor, D, in a locally isotropic medium, with an accommodation made for different orthogonal transverse dispersivity values, can be expressed as [*Burnett and Frind*, 1987]

$$\begin{aligned} D_{xx} &= \left(\alpha_L v_x^2 + \alpha_{TH} v_y^2 + \alpha_{TV} v_z^2\right)/|v| + D^*, \\ D_{yy} &= \left(\alpha_L v_y^2 + \alpha_{TH} v_x^2 + \alpha_{TV} v_z^2\right)/|v| + D^*, \\ D_{zz} &= \left(\alpha_L v_z^2 + \alpha_{TH} v_x^2 + \alpha_{TV} v_y^2\right)/|v| + D^*, \\ D_{xy} &= D_{yx} = (\alpha_L - \alpha_{TH}) v_x v_y/|v|, \\ D_{xz} &= D_{zx} = (\alpha_L - \alpha_{TV}) v_x v_z/|v|, \\ D_{yz} &= D_{zy} = (\alpha_L - \alpha_{TV}) v_y v_z/|v|, \end{aligned} \tag{2}$$

where v_x, v_y, and v_z are the components of the pore water velocity v and $|v|$ is its magnitude; α_L is the longitudinal dispersivity; α_{TH} and α_{TV} are the transverse dispersivities in the horizontal and vertical directions, respectively; D^* is the molecular diffusion coefficient in porous media.

[11] Because of the uncertainty associated with the hydraulic conductivity (or permeability), the hydraulic head and pore water velocity become stochastic, and so does the concentration of the solute that is moved by flow. The external sink/source term $q_s C_s$ is assumed to be deterministic. The objective of this work is to solve for the mean solute concentration and the uncertainty associated with the mean prediction through the concentration variance. Stochastic solutions of flow problems using the KLME approach can be found in our previous works [e.g., *Zhang and Lu*, 2004; *Lu and Zhang*, 2004; *Liu et al.*, 2006] and are thus not repeated here.

2.2. Karhunen-Loève Expansion-Based Moment Equations

[12] To solve (1) using the KLME approach, we first expand the stochastic variables C, D, v into infinite series,

$$C = \sum_{m=0}^{\infty} C^{(m)}, \quad D = \sum_{m=0}^{\infty} D^{(m)}, \quad v = \sum_{m=0}^{\infty} v^{(m)}, \tag{3}$$

where $C^{(m)}$, $D^{(m)}$ and $v^{(m)}$ are the mth-order expansions with respect to the standard deviation of log hydraulic conductivity, σ_Y. The detailed expressions of $v^{(m)}$ related to the variability of hydraulic head and hydraulic conductivity are given by *Lu and Zhang* [2004]. The derivations of $D^{(m)}$ up to the third order are provided in Appendix A. It is noteworthy that in some previous studies [e.g., *Kapoor and Gelhar*, 1994a, 1994b; *Zhang and Neuman*, 1996; *Hu et al.*, 1999; *Morales-Casique et al.*, 2006a, 2006b], the dispersion tensor D has been treated as given constants or linear functions of mean flow velocities, and therefore the effects of velocity variations on D are disregarded arbitrarily. As will be demonstrated in the following sections, this approximation, equivalent to using $D^{(0)}$ to approximate D in (3), may become problematic in certain cases where higher-order $D^{(m)}$ arising from the velocity fluctuations are significant.

[13] Substituting (3) into (1a) and rearranging the summations, one obtains

$$\sum_{m=0}^{\infty} \frac{\partial C^{(m)}}{\partial t} = \sum_{m=0}^{\infty} \sum_{k=0}^{m} \nabla \cdot \left(D^{(k)} \nabla C^{(m-k)}\right) - \sum_{m=0}^{\infty} \sum_{k=0}^{m} \nabla \cdot \left(v^{(k)} C^{(m-k)}\right) + q_s C_s. \tag{4}$$

Note that the external sink/source term is assumed to be deterministic and can thus be grouped with zeroth-order terms (relaxing this assumption is straightforward [*Zhang*, 2002]). One can separate (4) at different expansion orders with respect to σ_Y:

zeroth order:

$$\frac{\partial C^{(0)}}{\partial t} = \nabla \cdot \left(D^{(0)} \nabla C^{(0)}\right) - \nabla \cdot \left(v^{(0)} C^{(0)}\right) + q_s C_s, \tag{5a}$$

subject to the initial and boundary conditions

$$C^{(0)}(\boldsymbol{x}, 0) = C_0(\boldsymbol{x}), \qquad \boldsymbol{x} \in \Omega, \tag{5b}$$

$$C^{(0)}(\boldsymbol{x}, t) = C_D(\boldsymbol{x}, t), \qquad \boldsymbol{x} \in \Gamma_D, \tag{5c}$$

$$D^{(0)} \nabla C^{(0)} \cdot \boldsymbol{n}(\boldsymbol{x}) = -F, \qquad \boldsymbol{x} \in \Gamma_N. \tag{5d}$$

first order:

$$\frac{\partial C^{(1)}}{\partial t} = \nabla \cdot \left(D^{(0)} \nabla C^{(1)}\right) - \nabla \cdot \left(v^{(0)} C^{(1)}\right) + g^{(1)}, \tag{6a}$$

subject to

$$C^{(1)}(\boldsymbol{x}, 0) = 0, \qquad \boldsymbol{x} \in \Omega, \tag{6b}$$

$$C^{(1)}(\boldsymbol{x}, t) = 0, \qquad \boldsymbol{x} \in \Gamma_D, \tag{6c}$$

$$D^{(0)} \nabla C^{(1)} \cdot \boldsymbol{n}(\boldsymbol{x}) = -D^{(1)} \nabla C^{(0)} \cdot \boldsymbol{n}(\boldsymbol{x}), \qquad \boldsymbol{x} \in \Gamma_N, \tag{6d}$$

where

$$g^{(1)} = \nabla \cdot \left(D^{(1)} \nabla C^{(0)} - v^{(1)} C^{(0)}\right). \tag{6e}$$

Similarly one can derive the equations at higher expansion orders. Refer to Appendix B for the equations at the second, third and general mth orders, $m \geq 1$. Equations (5)–(6), and (B1)–(B9) are in principle equivalent to the formulations solved by *Hu et al.* [1999] except that our equations have been reformulated into the original form (1) with the stochastic D and v replaced by the deterministic zeroth-order terms $D^{(0)}$ and $v^{(0)}$. The terms involving higher-order $D^{(m)}$ and $v^{(m)}$ at $m \geq 1$ are lumped into the randomness terms $g^{(m)}$.

[14] Unlike that of *Hu et al.* [1999], in the KLME method the higher-order stochastic expansions (6), and (B1)–(B9)

are not used explicitly to formulate the corresponding moment equations, which can lead to a large dimensionality as mentioned in section 1. Instead, $C^{(m)}$, $D^{(m)}$ and $v^{(m)}$ are further expanded in terms of orthogonal standard random variables,

$$C^{(m)} = \sum_{i_1,i_2,\ldots,i_m=1}^{\infty} \left(\prod_{j=1}^{m} \xi_{i_j}\right) C^{(m)}_{i_1,i_2,\ldots,i_m},$$
$$D^{(m)} = \sum_{i_1,i_2,\ldots,i_m=1}^{\infty} \left(\prod_{j=1}^{m} \xi_{i_j}\right) D^{(m)}_{i_1,i_2,\ldots,i_m}, \quad (7)$$
$$v^{(m)} = \sum_{i_1,i_2,\ldots,i_m=1}^{\infty} \left(\prod_{j=1}^{m} \xi_{i_j}\right) v^{(m)}_{i_1,i_2,\ldots,i_m},$$

where $C^{(m)}_{i_1,i_2,\ldots,i_m}$, $D^{(m)}_{i_1,i_2,\ldots,i_m}$ and $v^{(m)}_{i_1,i_2,\ldots,i_m}$ are all deterministic functions to be determined; i_1, i_2, $\cdots$, i_m are referred to as the expansion modes at the mth order; ξ_{i_j} are the orthogonal standard random variables. For instances, up to the third order, $C^{(1)}$, $C^{(2)}$ and $C^{(3)}$ are expanded as

$$C^{(1)} = \sum_{i_1=1}^{\infty} \xi_{i_1} C^{(1)}_{i_1}, C^{(2)} = \sum_{i_1,i_2=1}^{\infty} \xi_{i_1}\xi_{i_2} C^{(2)}_{i_1,i_2},$$
$$C^{(3)} = \sum_{i_1,i_2,i_3=1}^{\infty} \xi_{i_1}\xi_{i_2}\xi_{i_3} C^{(3)}_{i_1,i_2,i_3}. \quad (8)$$

As shown by *Lu and Zhang* [2004] and in Appendix A, $D^{(m)}_{i_1,i_2,\ldots,i_m}$ and $v^{(m)}_{i_1,i_2,\ldots,i_m}$ can be calculated after stochastic head solutions are obtained. $C^{(m)}_{i_1,i_2,\ldots,i_m}$ are the quantities to be solved for in this work as they provide the basis to compute both the mean concentration and concentration variance (as well as other higher concentration moments, if desired).

[15] Substituting (7) into (6) and then dropping the independent set $\{\xi_i\}$, one obtains the following equations for $C^{(1)}_{i_1}$ at the first-order mode i_1,

$$\frac{\partial C^{(1)}_{i_1}}{\partial t} = \nabla \cdot \left(D^{(0)} \nabla C^{(1)}_{i_1}\right) - \nabla \cdot \left(v^{(0)} C^{(1)}_{i_1}\right) + g^{(1)}_{i_1}, \quad (9a)$$

subject to

$$C^{(1)}_{i_1}(\boldsymbol{x}, 0) = 0, \qquad \boldsymbol{x} \in \Omega, \quad (9b)$$

$$C^{(1)}_{i_1}(\boldsymbol{x}, t) = 0, \qquad \boldsymbol{x} \in \Gamma_D, \quad (9c)$$

$$D^{(0)} \nabla C^{(1)}_{i_1} \cdot n(\boldsymbol{x}) = -D^{(1)}_{i_1} \nabla C^{(0)} \cdot \boldsymbol{n}(\boldsymbol{x}), \qquad \boldsymbol{x} \in \Gamma_N, \quad (9d)$$

where

$$g^{(1)}_{i_1} = \nabla \cdot \left(D^{(1)}_{i_1} \nabla C^{(0)} - v^{(1)}_{i_1} C^{(0)}\right). \quad (9e)$$

Similarly one can derive the equations for $C^{(m)}_{i_1,i_2,\ldots,i_m}$ at higher expansion orders and modes. Refer to Appendix B for the equations at the second-, third-, and general mth-order modes i_1, i_2, $\cdots$, i_m, $m \geq 1$.

[16] Once the deterministic coefficients $C^{(m)}_{i_1,i_2,\ldots,i_m}$ are solved, one can easily compute the mean concentration and concentration variance by some simple algebraic operations. For example, up to the third order in σ_Y,

$$C \approx \sum_{m=0}^{3} C^{(m)}, \quad (10)$$

and the mean concentration can be approximated as

$$\langle C \rangle \approx \sum_{m=0}^{3} \langle C^{(m)} \rangle = C^{(0)} + \langle C^{(2)} \rangle = C^{(0)} + \sum_{i_1=i_2=1}^{\infty} C^{(2)}_{i_1,i_2}, \quad (11)$$

where the first term in the right-hand side is the zeroth-order mean concentration solution and the second term represents the second-order correction in σ_Y. The terms $C^{(2)}_{i_1,i_2}$ for $i_1 \neq i_2$ disappear because $\langle \xi_{i_1}\xi_{i_2} \rangle$ is equal to zero. The first-order correction is not involved because $\langle \xi_{i_1} \rangle$ is equal to zero.

[17] From (10) and (11), one can write the perturbation term up to the third order in σ_Y as,

$$C' = C - \langle C \rangle \approx \sum_{m=1}^{3} C^{(m)} - \sum_{i_1=i_2=1}^{\infty} C^{(2)}_{i_1,i_2}. \quad (12)$$

The concentration variance can be calculated by squaring (12) and then taking the ensemble mean,

$$\sigma^2_C \approx \sum_{i_1=1}^{\infty} \left[C^{(1)}_{i_1}\right]^2 + 2 \sum_{i_1,i_2=1}^{\infty} \left[C^{(2)}_{i_1,i_2}\right]^2 + 6 \sum_{i_1,i_2=1}^{\infty} \left[C^{(1)}_{i_1} C^{(3)}_{i_1,i_2,i_2}\right], \quad (13)$$

where the first term on the right-hand side is the concentration variance up to the first order in the variance of log conductivity σ^2_Y, and the second and third terms represent the second-order corrections in σ^2_Y.

[18] Equations (5), (9), and (B10)–(B18) have the same structure as the original transport equation (1). Therefore any existing simulator, such as Modular Three-Dimensional Multispecies Transport Model for Simulation of Advection, Dispersion, and Chemical Reactions of Contaminants in Groundwater Systems (MT3DMS) [*Zheng and Wang*, 1999], can be directly used to solve $C^{(m)}_{i_1,i_2,\ldots,i_m}$. Moreover, because of the same structure of these equations, the left-hand-side coefficient matrix remains unchanged across simulator calculations for different expansion orders and modes, which further allows us to increase the computational efficiency of the KLME approach. Because of the recursive nature, solving (5), (9), and (B10)–(B18) is a sequential process from low to high expansion orders. At the same order, the equations are independent of each other, a feature that enables potential parallel computing for large-scale problems. In this work, $C^{(m)}_{i_1,i_2,\ldots,i_m}$ is evaluated up to the third order. The appropriate solution procedure is (1) at the current time step, solve the zeroth-order equation (5) for $C^{(0)}$, (2) solve (9) for $C^{(1)}_{i_1}$ at the first-order mode i_1, (3) continue to solve (B10)–(B13) for the $C^{(2)}_{i_1,i_2}$ at the second-order mode i_1, i_2 and $C^{(3)}_{i_1,i_2,i_3}$ at the third-order mode i_1, i_2, i_3, (4) compute the mean and variance of concentration using (11) and (13), and (5) add a time increment and repeat steps 1–4, if needed. In step 5 where the KLME calculations reach the next transport step, if the flow field is

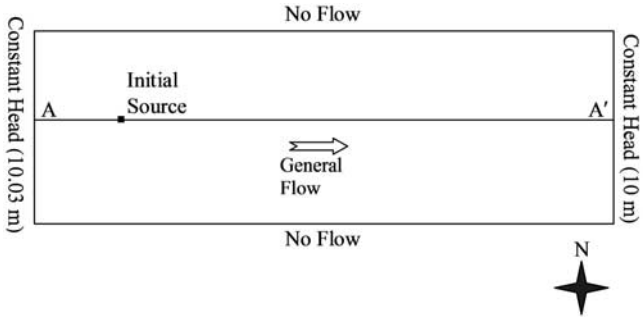

Figure 1. Schematic diagram of model setup in the 2-D examples. Line A-A′ indicates where the simulation results are compared between the KLME and MC approaches in details.

transient, the flow velocities at the new time should be read in and used in steps 1–4. A new code called "MT3DMS-STO" has been developed to implement numerically the stochastic formulation presented here, in which MT3DMS is employed as a subroutine to calculate $C^{(m)}_{i_1,i_2,\ldots,i_m}$ at different expansion orders m and modes $i_1, i_2, \cdots, i_m$.

3. Illustrative Examples

[19] The validity of the KLME approach for stochastic uncertainty analysis in solute transport problems is evaluated through a series of 2-D numerical experiments. Results from the proposed KLME methodology are compared to those from the classical MC simulations. The log-transformed random hydraulic conductivity field is assumed to be second-order stationary and follows a separable exponential covariance function,

$$C_Y(\boldsymbol{x}_1, \boldsymbol{x}_2) = \sigma_Y^2 \exp\left[-\frac{|x_1 - x_2|}{\eta_x} - \frac{|y_1 - y_2|}{\eta_y}\right], \qquad (14)$$

where $\boldsymbol{x}_1 = (x_1, y_1)^{\mathrm{T}}$ and $\boldsymbol{x}_2 = (x_2, y_2)^{\mathrm{T}}$ are any two points in the simulation domain, η_x and η_y are the correlation lengths in x and y directions, respectively. In the following examples, the correlation lengths are set to $\eta_x = \eta_y = 1$ m, and the variance σ_y^2 varies from 0.5 to 1.5.

3.1. Numerical Model Setup

[20] The flow and transport domain is 30 m long by 10 m wide (Figure 1). There is no flow across the northern (top) and southern (bottom) boundaries; on the western (left) and eastern (right) boundaries the hydraulic heads are prescribed as constant at 10.03 and 10 m, respectively, such that an average hydraulic gradient of 0.001 is achieved in the mean flow direction. The model is discretized into a block-centered finite difference grid of 121 columns and 40 rows with uniform cell dimensions of 0.25 m by 0.25 m (one extra column added to because of the particular eastern and western boundary configurations). As a result, one correlation length of log conductivity occupies 4 individual cells. The simulated flow field is confined and steady state.

[21] In the transport simulations, zero concentration gradient is specified across all four boundaries (the dispersive boundary flux F is zero). The local dispersivity in the longitudinal direction α_L is set equal to 0.2 m while the dispersivity ratio between transverse and longitudinal directions (α_{TH}/α_L) remains constant at 0.1. All simulations employ a uniform effective porosity of 0.35, and a molecular diffusion coefficient of 5.0×10^{-4} m^2/d. The initial mass is distributed into a single cell and placed on the central west-east line, 4.5 m downstream from the western border (Figure 1). Line A-A′ indicates where the simulation results will be analyzed in details.

3.2. KLME and Classical MC Approaches

[22] As mentioned earlier, in the KLME approach we obtained the solutions of $C^{(m)}_{i_1,i_2,\ldots,i_m}$ up to the third order, namely, $C^{(0)}$, $C^{(1)}_{i_1}$, $C^{(2)}_{i_1,i_2}$ and $C^{(3)}_{i_1,i_2,i_3}$. In the following examples $C^{(1)}_{i_1}$ are calculated for the first 100 modes, $i_1 = \overline{1,100}$ at the first order; at the second order, $C^{(2)}_{i_1,i_2}$ are calculated for the first 30 by 30 modes, i_1 , $i_2 = \overline{1,30}$; and at the third order, $C^{(3)}_{i_1,i_2,i_3}$ are calculated for the first 20 by 20 by 20 modes, i_1, i_2, $i_3 = \overline{1,20}$. The numbers of modes here are chosen sufficiently large so that the statistics of $C^{(m)}_{i_1,i_2,\ldots,i_m}$ converges at the respective expansion order m. In order to achieve both the computational efficiency and accuracy, the optimal combination of the mode numbers at different orders may vary from case to case, depending on the specific model setting and conductivity statistics under consideration. Compared to those in the flow cases [*Zhang and Lu*, 2004; *Liu et al.*, 2006], a larger number of modes are typically needed to assure the statistical convergence in the KLME transport approach. The effects of the mode numbers will be further examined in the following sections.

[23] As in the study by *Liu et al.* [2006], the mode coefficients of the hydraulic head, $h^{(m)}_{i_1,i_2,\ldots,i_m}$, are solved by MODFLOW-2000 [*Harbaugh et al.*, 2000]. For the mode coefficients of solute concentration, $C^{(m)}_{i_1,i_2,\ldots,i_m}$, MT3DMS is applied as a solver. Note that the KLME is essentially a concentration gradient-based approach and therefore it is particularly susceptible to numerical oscillation. As such, all the transport terms are solved by an implicit General Conjugate-Gradient (GCG) method in MT3DMS. To further ensure numerical accuracy, the transport time step is bounded by a Courant number of 0.50.

[24] In the MC simulations, 5000 realizations of the conductivity field are used. The conductivity fields are generated using the KL decomposition technique [*Zhang and Lu*, 2004] with the leading 2000 eigenvalues and eigenfunctions. MODFLOW-2000 and MT3DMS are applied repeatedly to simulate the corresponding concentration solution for each conductivity realization. Upon the completion of 5000 simulations, the ensemble statistics of solute concentration is calculated as,

$$\langle C \rangle \approx \frac{1}{5000} \sum_{k=1}^{5000} C_k, \qquad (15)$$

$$\sigma_C^2 \approx \frac{1}{4999} \sum_{k=1}^{5000} (C_k - \langle C \rangle)^2, \qquad (16)$$

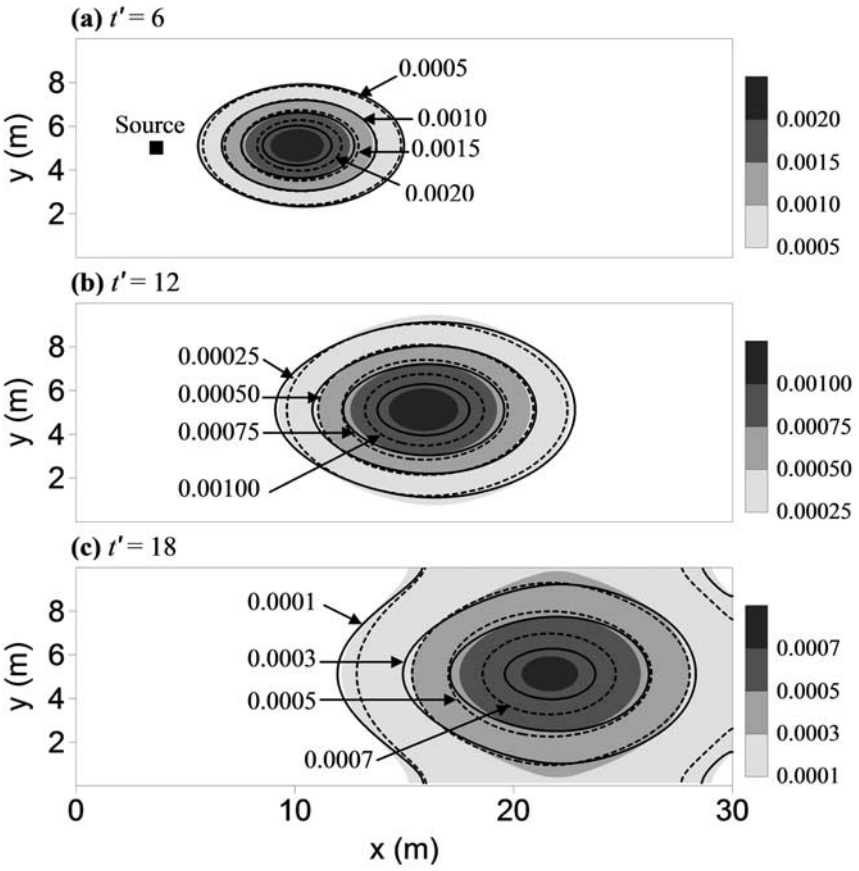

Figure 2. Normalized mean concentration ($\langle C/C_0 \rangle$) calculated from the MC simulations and KLME approach at three different times: (a) $t' = 6$, (b) $t' = 12$, and (c) $t' = 18$. C_0 is the initial source concentration. The filled contours stand for the result from MC simulations, the dashed lines stand for the zeroth-order solution, and the solid lines stand for the result after the second-order correction in the KLME approach. For reference, the initial source is also shown in Figure 2a.

where C_k is the simulated solute concentration for conductivity realization k.

3.3. Results and Discussions

3.3.1. Case for $\sigma_Y^2 = 0.5$

[25] In this case we consider a log conductivity variance σ_Y^2 of 0.5, which can be converted to a coefficient of variation of 80.5% for the original conductivity field before the log transformation. The flow field is driven by the influx across the western border and no other external stresses are involved. Figure 2 displays the contours of mean concentration from both MC simulations, i.e., (15), and the KLME approach, i.e., (11), at different dimensionless times. The dimensionless time is defined as $t' = \langle v_x \rangle \, t/\eta_x$, which describes the number of correlation lengths the solute plume has traveled in the mean flow direction up to time t.

[26] Figure 2 indicates that compared to the MC solution, the zeroth-order KLME result, which is based only on the geometric mean conductivity field, overestimates solute spreading at the plume center while shows underestimation toward the edges of plume. By adding the second-order correction, i.e., the second term in (11), the result is much improved and the match between the KLME approach and MC simulations becomes significantly better. The accuracy of the second-order KLME result to resemble those from MC simulations is consistently good in both the transverse and longitudinal directions through different times.

[27] As shown in (13), an obvious advantage of the KLME approach is the ease at which the concentration variance can be estimated by simple algebraic operations on the mode expansions $C^{(m)}_{i_1,i_2,\ldots,i_m}$. Figure 3 plots the concentration variance calculated by the KLME approach and MC simulations at different times for the same model settings as in Figure 2. To facilitate visual observations, only the second-order KLME result (i.e., with all three terms in (13)) is presented. It can be seen that despite some local mismatch, the overall concentration variability estimated from the KLME approach is in good agreement with the MC solution. The concentration variance is bimodal in the flow direction, indicating that the solute concentration has the largest variability in the limbs of plume where the concentration gradient is relatively high. The bimodal concentration variance behavior was also observed by others [e.g., *Zhang and Neuman*, 1996; *Rubin*, 2003; *Morales-Casique et al.*, 2006b].

[28] Figure 4 shows the mean concentration and concentration variance along the profile A-A′. Being consistent with the contours in Figure 2, the zeroth-order KLME concentration shows a peak that is higher than that from MC simulations and underpredicts the solute spreading in

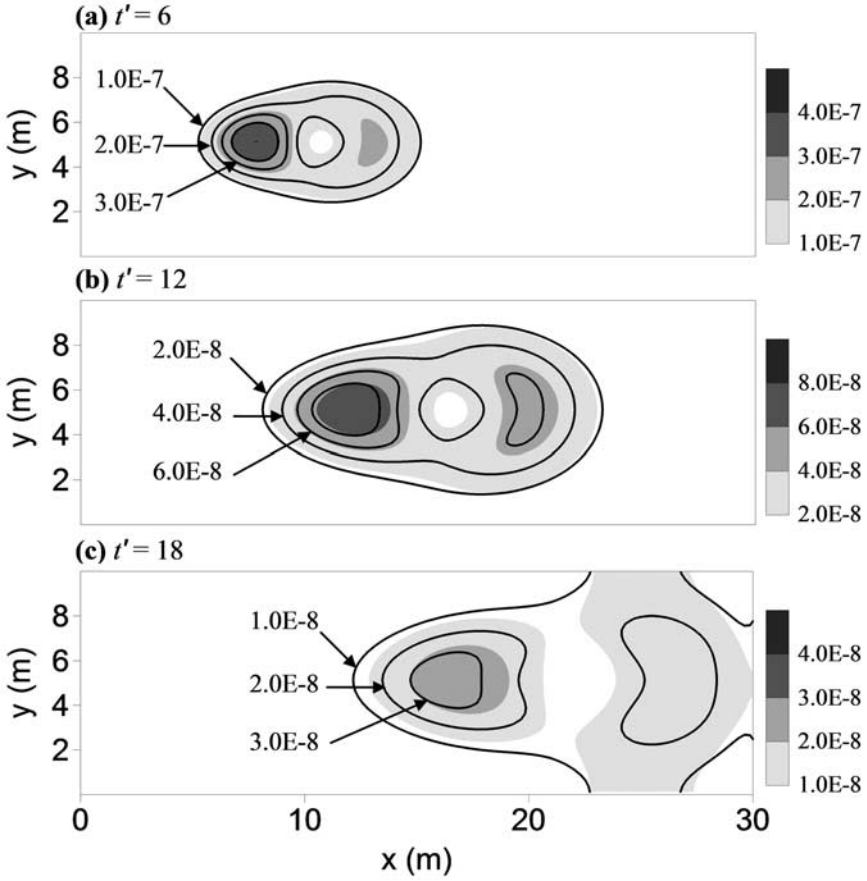

Figure 3. Concentration variance (σ^2_{C/C_0}) calculated from the MC simulations and KLME approach at three different times: (a) $t' = 6$, (b) $t' = 12$, and (c) $t' = 18$. To facilitate the visual comparison, only the second-order result is provided in the KLME approach.

the areas toward the outside plume edges. The second-order KLME concentration shows a significant improvement over the zeroth-order result and matches the solution from MC simulations very well at both the plume center and outside edges. The accuracy of the KLME approach is well preserved through different times. For the concentration variance, the first-order KLME result, which is based on the first term in (13) only, overshoots the bimodal peaks from MC simulations and undershoots the low values at plume center. The second-order correction, i.e., the second and third terms in (13), improves the solution accuracy by rectifying both the overestimation at the peaks and the underestimation at the middle low values. Compared to the mean concentration, the second-order improvement on the concentration variance is to a lesser degree.

3.3.2. Effects of Mode Numbers

[29] In section 3.2 we mentioned that the mode numbers at different expansion orders were specified a priori and remained constant across different cases, although the optimal combination of mode numbers could vary depending on the specific model setting and conductivity statistics under consideration. Here we further investigate the effects of mode numbers upon the concentration statistics in the KLME approach. Figure 5 shows the mean concentration calculated with different second-order mode numbers at $t' = 12$ and $\sigma^2_Y = 0.5$ in the KLME approach. The model settings in generating Figure 2 are used here. The effects of mode numbers upon the concentration variance are not provided here, because the computation of concentration variance involves the modes from all the first three expansion orders and a straightforward evaluation cannot be readily made. Figure 5 indicates that the second-order correction on the mean concentration is most significant during the first 20 modes, and thereafter the mode contribution decreases progressively. Clearly, the computational effort can be further reduced in the KLME approach by taking into account only those modes that are contributing significantly.

3.3.3. Case for $\sigma^2_Y = 1.0$

[30] In this section we explore the performance of the KLME approach when the conductivity variance σ^2_Y is increased to 1.0. The corresponding coefficient of variation is 131.1% for the original conductivity field. Other settings remain identical to those in Figure 1. Figure 6 displays the mean concentration and concentration variance calculated by the KLME approach and MC simulations at $\sigma^2_Y = 1.0$. It is seen that when the conductivity variance increases to 1.0, the mean concentration is still accurately reproduced by the KLME approach. For the concentration variance, however, the mismatch between the KLME approach and MC simulations becomes significant especially at the plume center. The second-order KLME correction largely overpredicts the low values between the bimodal peaks from MC simulations.

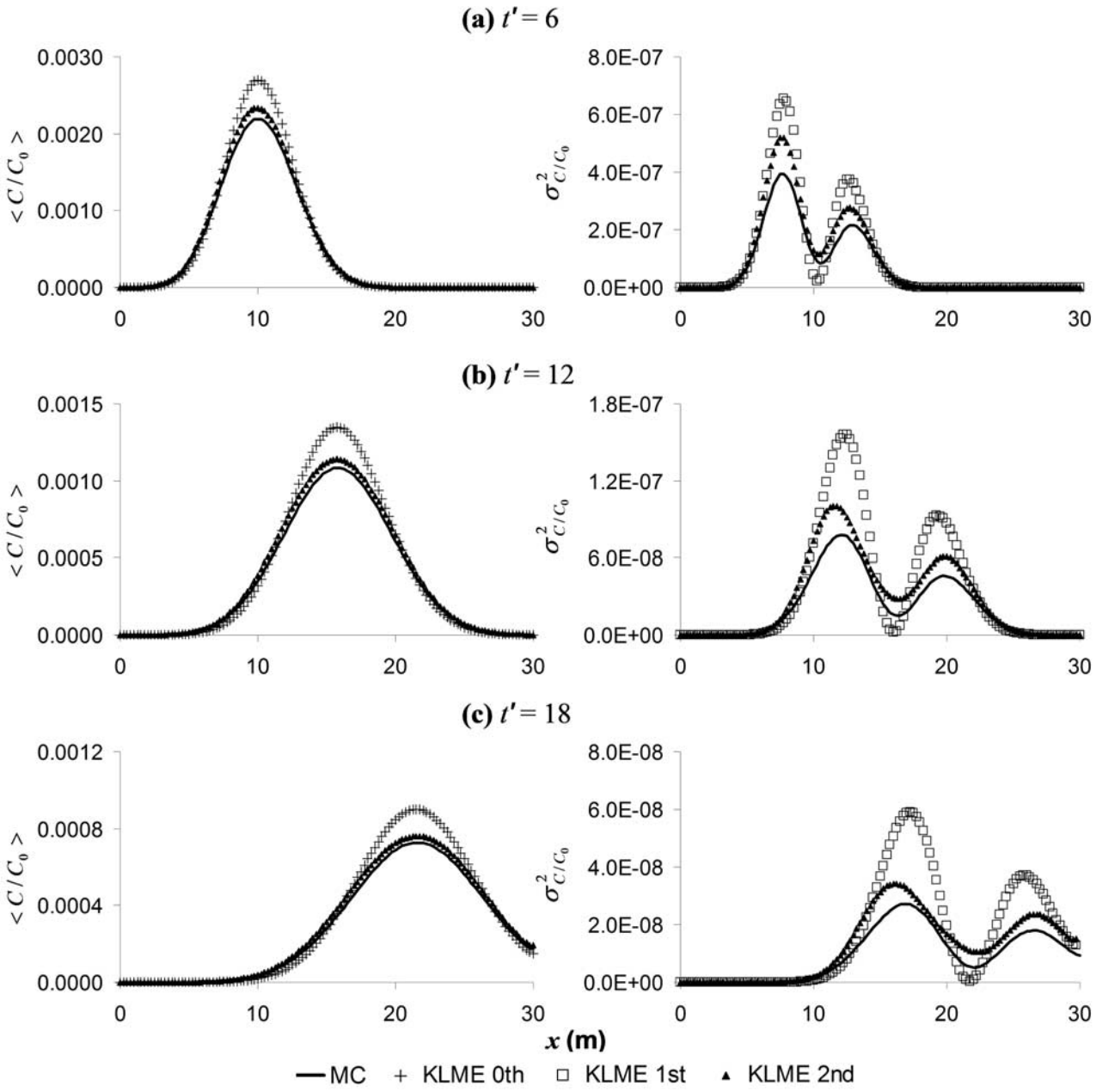

Figure 4. Mean and variance of concentration along the profile A-A′ at three different times in Figure 2: (a) $t' = 6$, (b) $t' = 12$, and (c) $t' = 18$.

[31] When the conductivity variance is large, the inadequacy of perturbative approaches to estimate the concentration variance has been also been documented in some recent literature [e.g., *Morales-Casique et al.*, 2006b; *Neuman*, 2006]. The KLME approach developed in this paper has been shown to be effective for predicting the concentration variance when the conductivity variance is 0.5, but becomes problematic when the conductivity variance increases to 1.0. *Morales-Casique et al.* [2006b] reported that their iterative perturbative solutions of the concentration variance were only applicable for $\sigma_Y^2 < 0.3$. Conceivably, this limitation can be potentially overcome by the new multiscale decomposition approach proposed by *Neuman* [2006].

[32] Because of the loss of accuracy on the concentration variance, the KLME approach is suggested mainly as a tool for evaluating the mean concentration when the conductivity variance is 1.0 or larger. Additional simulations (not reported here) indicate that the mean concentration calculated by the KLME approach remains accurate at $\sigma_Y^2 < 1.5$ and the mismatch error starts to elevate when σ_Y^2 is 1.5 or larger.

3.3.4. Computational Efforts in KLME

[33] The computational efforts in the KLME approach are directly proportional to the number of mode coefficients $C^{(m)}_{i_1,i_2,\ldots,i_m}$ involved at each expansion order m. As mentioned in section 3.2, to compute the mean concentration and concentration variance, we used 100, 30 by 30 and 20 by 20

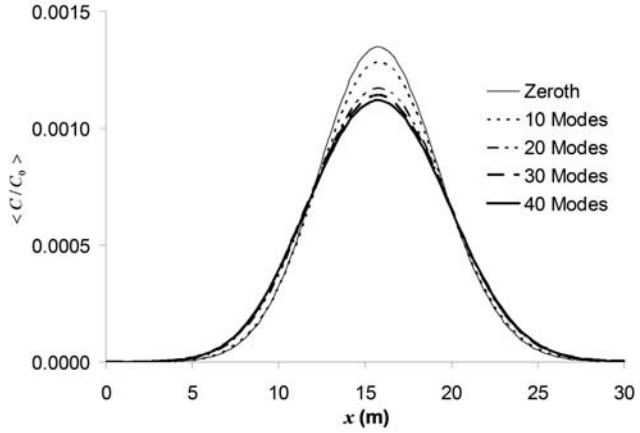

Figure 5. Mean concentration calculated with different second-order mode numbers at $t' = 12$ in the KLME approach. Model settings are identical to those in Figure 1.

by 20 modes at the first, second and third orders, respectively. The total number of mode calculations (plus the zeroth-order $C^{(0)}$) is 1676. For both $\sigma_Y^2 = 0.5$ and 1.0, the actual CPU time taken by the KLME approach was about 11 hours on a Xeon(TM)-PC equipped with a 3.20 GHz processor with 1 Gb of memory. In the MC simulations, it took about 17 hours to finish the simulation of 5000 realizations for $\sigma_Y^2 = 0.5$, and about 22 hours for $\sigma_Y^2 = 1.0$. In the KLME approach, different mode calculations are always conducted on the smooth geometrical mean conductivity field. As a result, the CPU time does not change with the conductivity variance. In the MC simulations, however, the conductivity variability in each realization increases as the variance becomes large. Correspondingly, the CPU time increases as the transport step size is constrained by the Courant number 0.5.

[34] It should be pointed out that when the KLME approach is used only to predict the mean concentration, the computational efforts can be reduced dramatically as the mode calculations at the third expansion order are not needed anymore. For instance, if 30 by 30 modes at the second expansion order are used in estimating the mean concentration, the total number of mode calculations is 1 (zeroth order) + 30 (first order, not directly involved in the mean concentration but needed in the second-order mode calculations) + 30 (second order, the off-diagonal mode coefficients $C^{(2)}_{i_1,i_2}$ for $i_1 \neq i_2$ not involved in the mean concentration) = 61. In other words, while a total of 1676 mode coefficients are used to compute the mean and variance of concentration in the KLME approach, only 61 of them are involved for computing the mean concentration. In addition, as shown in section 3.2.2, the number of modes required may be further reduced by taking in account only those modes that are contributing significantly.

[35] Because the structure of the mode coefficient equations (i.e., (5), (9), and (B10)–(B18)) is the same at different orders and modes, the left-hand side coefficient matrix involved in each MT3DMS subroutine calculation remains identical. This feature can further allow us to significantly reduce the computational efforts required by the KLME approach. Similar to the MC simulations, parallel computing is possible in the KLME approach as the mode equations are independent of one another at each expansion order.

3.3.5. Higher-Order Dispersion Terms

[36] As mentioned earlier, unlike some previous studies [*Kapoor and Gelhar*, 1994a, 1994b; *Zhang and Neuman*, 1996; *Hu et al.*, 1999; *Morales-Casique et al.*, 2006a, 2006b] where the local dispersion has been treated as given constants or simple functions of mean velocities, here we consider the effects of velocity variations upon local dispersion by including the higher-order $D^{(m)}$ terms in the KLME formulation. Figure 7 compares the mean concentration calculated by the KLME approach between the case where only the zeroth-order dispersion term $D^{(0)}$ is used and the case where the higher-order terms $D^{(1)}$, $D^{(2)}$, and $D^{(3)}$ are also included. For $\sigma_Y^2 = 0.5$, the mean concentration does not change much after including the higher-order dispersion terms and all the results are in excellent agreement with each other. For $\sigma_Y^2 = 1.0$, however, the mean concentration without considering the contributions of higher-order dispersion terms is apparently asymmetric and skews toward the downgradient side of plume center. Clearly, when the conductivity variance increases, the effects of the higher-order dispersion terms become more significant and a rigorous treatment of the dispersion terms is more appropriate.

3.3.6. Presence of Pumping Well

[37] To explore the performance of the KLME approach under the influence of external stresses, a pumping well is

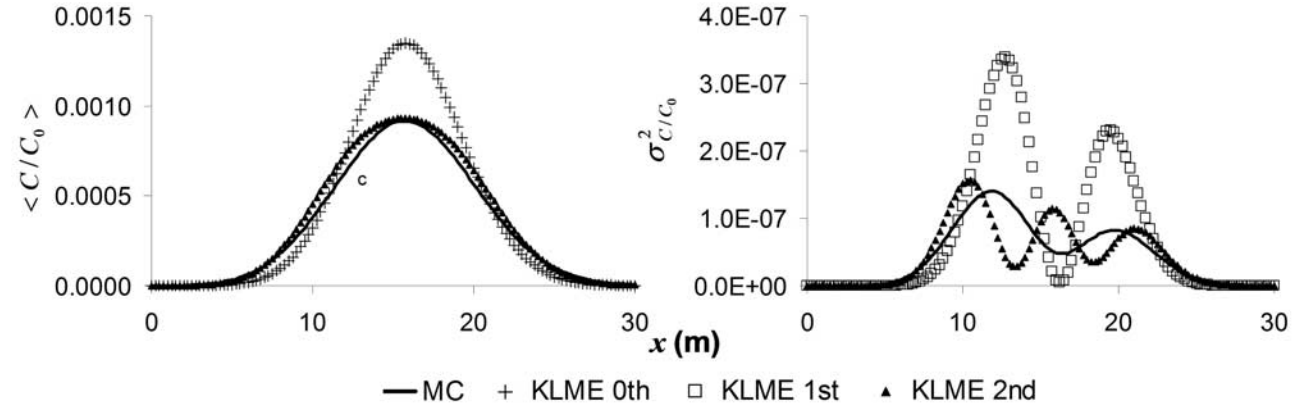

Figure 6. Mean and variance of concentration along the profile A-A′ at t′ = 12 when σ_Y^2 is increased to 1.0.

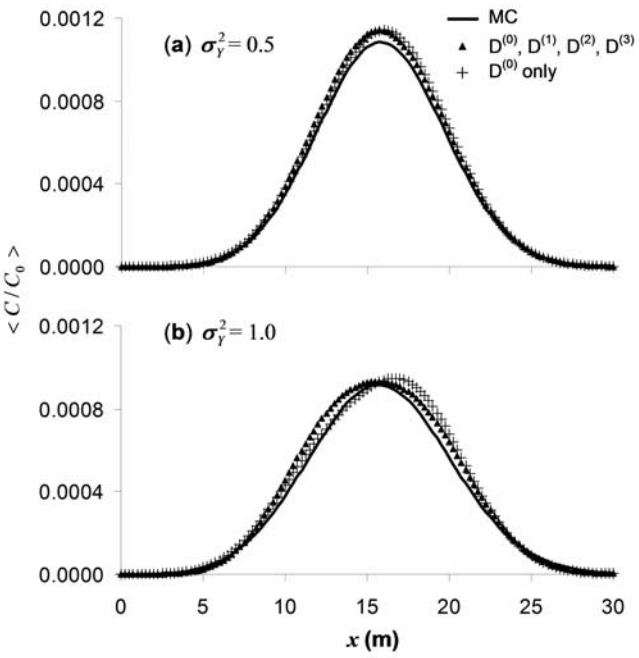

Figure 7. Mean concentration calculated by the KLME approach between the case where only the zeroth-order dispersion term $D^{(0)}$ is used and the case where the higher-order terms $D^{(1)}$, $D^{(2)}$, and $D^{(3)}$ are also included at (a) $\sigma_Y^2 = 0.5$ and (b) $\sigma_Y^2 = 1.0$. Results are shown for $t' = 12$.

added and placed at the center of domain with a pumping rate of 1.0 m^3/d (Figure 8). An observation well is also installed at 5 m upstream of the pumping well. The conductivity variance is 0.5. The zeroth-order concentration at $t' = 3$ for the case in Figure 2 is applied as the distributed initial source. Other model settings remain identical to those in Figure 1. It is noteworthy that the computational efforts in the MC simulations are increased dramatically by including the pumping well. The CPU time for completing the simulation of 5000 realizations in the MC simulations is 108.5 hours, significantly longer than 16.5 hours in the KLME approach.

[38] Figure 8 displays the head contours after the pumping well is included. The flow field is based on the geometric mean conductivity in the KLME approach. The hydraulic head and velocity are significantly altered by the pumping well as compared to those in the previous cases. Note that after adding a pumping well, the flow velocity field becomes strongly nonstationary even though the underlying conductivity is specified as second-order stationary.

[39] Figure 9 shows the mean concentration and concentration variance calculated at the pumping and observation wells through different times. For the mean concentration, the zeroth-order KLME result overshoots the values calculated from the MC simulations at both wells and the second-order correction improves the solution accuracy significantly. For the concentration variance, the first-order KLME result overshoots both peaks at the pumping well and the second peak at the observation well, and the second-order correction yields a better agreement with the MC solution. It can be seen that the largest variability of solute concentration at both wells does not correspond to the mean concentration breakthrough peak. For instance, the first variance peak at the observation well appears shortly before the mean concentration peak arrival (~10 days), and the second peak shows up in later times after the main plume passes by (~25 days). This is because instead of at the plume center, the concentration fluctuation occurs most significantly at the limbs where the spatial gradient of solute concentration is largest.

4. Summary and Conclusions

[40] In this paper we have developed a new approach for solving subsurface solute transport problems in randomly heterogeneous media using the Karhunen-Loève-based moment equation (KLME) technique proposed by *Zhang and Lu* [2004]. The KLME approach is based on an innovative combination of the Karhunen-Loève (KL) decomposition of the underlying random conductivity field and the perturbative and polynomial expansions of dependent variables including the hydraulic head, flow velocity, dispersion coefficient, and solute concentration. The equations obtained in this approach are recursive and can be solved sequentially from low to high orders. The structure of these equations has been formulated in the same form as the original governing equations such that any existing simulator, such as MT3DMS [*Zheng and Wang*, 1999], can be directly applied as the solver. The theoretical derivations presented in this work have been numerically implemented in a code called "MT3DMS-STO."

[41] The validity of the KLME approach has been evaluated against the classical Monte Carlo (MC) simulations in a series of 2-D numerical experiments under different flow and transport conditions. Results indicated that the KLME approach yielded a good representation of the mean concentration from the MC simulations after the second-order correction at both the conductivity variance 0.5 and 1.0. Further simulations (not reported here) showed that the mismatch of the KLME approach on the mean concentration became elevated when the conductivity variance was 1.5 or larger. For the concentration variance, the KLME approach was effective in reproducing the MC solution at the conductivity variance 0.5. When the conductivity variance was increased to 1.0, the KLME approach generated noticeable errors as compared to the MC solution. As such, the KLME approach is suggested mainly as a tool for evaluating the mean concentration when the conductivity variance becomes large.

[42] When the conductivity variance is large, the inadequacy of perturbative approaches to estimate the concentration variance has also been documented in the recent

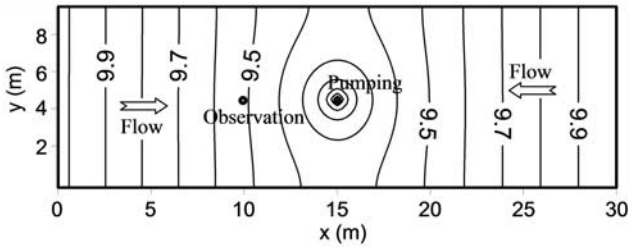

Figure 8. Head contours after the pumping well is turned on at a rate of 1.0 m^3/d. The flow field is based on the geometric mean conductivity in the KLME approach.

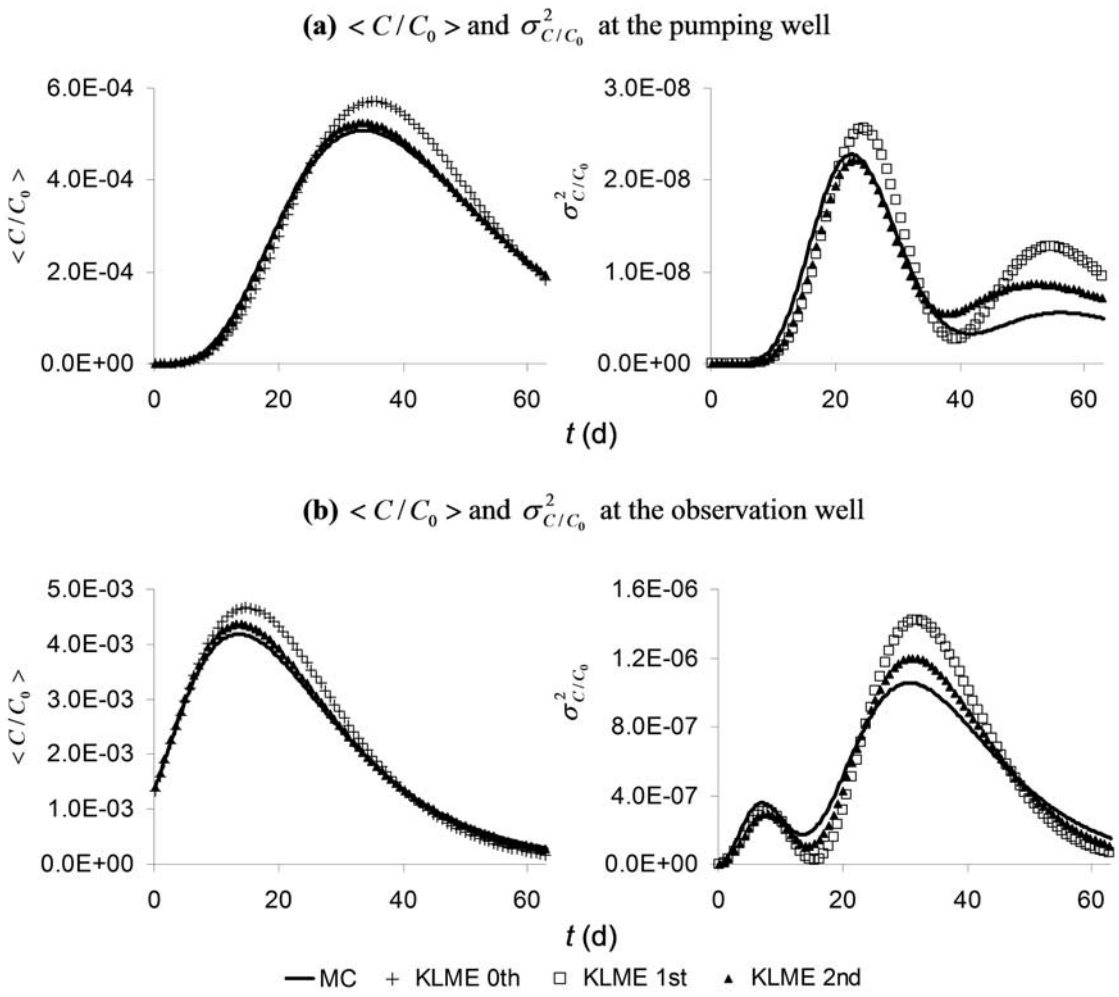

Figure 9. Breakthrough curves for the mean concentration and concentration variance at (a) the pumping well and (b) the observation well.

literature [e.g., *Morales-Casique et al.*, 2006b; *Neuman*, 2006]. *Morales-Casique et al.* [2006b] reported that their iterative perturbative solutions of the concentration variance were only applicable for $\sigma_Y^2 < 0.3$. Although the ensemble averaged plume behaviors have been characterized with success by various perturbation methods developed over the past two decades [*Gelhar et al.*, 1979; *Dagan*, 1984; *Neuman and Zhang*, 1990; *Hu et al.*, 1999; *Salandin and Fiorotto*, 2000; *Darvini and Salandin*, 2006], the applicability of the perturbative approaches to predict the concentration variance is still limited to small conductivity variance. That challenge remains open.

[43] Some specific conclusions can be drawn from the results of the 2-D examples considered in this work. First, compared to the MC solution, the zeroth-order mean concentration calculated by the KLME approach tends to overpredict at the plume center and underpredict at the outside plume edges. The second-order correction is able to rectify the mismatch in both areas. The accuracy of the mean concentration in the KLME approach is consistently good through different times. Second, the first-order concentration variance in the KLME approach tends to overestimate the bimodal peaks calculated by the MC simulations at the limbs of plume where the concentration gradient is largest. At the plume center, the concentration variance is small and the first-order KLME result shows some underestimation. When the conductivity variance is not large, the second-order KLME correction is able to improve the variance mismatch at both the peaks and middle low values. Third, when the conductivity variance is large, neglecting the higher-order dispersion terms can generate noticeable errors and a rigorous treatment of the dispersion terms becomes more appropriate. Fourth, the validity of the KLME approach maintains in the presence of a pumping well. Because of the pumping well, the flow velocity field becomes strongly nonstationary. Nonetheless, the KLME approach provides a fairly accurate estimation of the mean concentration and concentration variance at both the pumping and observation wells.

[44] It should be emphasized that the KLME approach provides considerable computational advantages as compared to the classical MC simulations as well as other perturbative techniques. Because the expanded equations at different orders and modes have the same structure as the original governing equations, any existing transport codes can be directly applied as the solver in the KLME approach. This

has not been possible in the traditional perturbative approaches where the integrodifferential moment equations are typically solved with the aid of some advanced transformations (e.g., Green's function). Compared to the MC simulations, the KLME approach requires much less computational effort when it is applied as the tool for computing the mean concentration only. In addition, while the CPU time in the MC simulations can increase significantly with the conductivity variance and in the presence of the pumping well, the computational effort in the KLME approach remains relatively unaffected as different mode coefficients are always evaluated on the geometric mean conductivity field.

Appendix A: Higher-Order Expansions of Dispersion Tensor *D*

[45] Let $W = 1/|v|$, $U_x = v_x^2$, $U_y = v_y^2$, $U_z = v_z^2$, $D_{xxL} = \alpha_L v_x^2/|v|$, $D_{xxTH} = \alpha_{TH} v_y^2/|v|$ and $D_{xxTV} = \alpha_{TV} v_z^2/|v|$, then

$$D_{xxL} = \alpha_L U_x W, D_{xxTH} = \alpha_{TH} U_y W, D_{xxTV} = \alpha_{TV} U_z W, \quad \text{(A1)}$$

and

$$D_{xx} = D_{xxL} + D_{xxTH} + D_{xxTV} + D^*. \quad \text{(A2)}$$

By approximating the pore water velocities up to the third order in σ_Y, W can be expanded as

$$\begin{aligned} W = 1/|v| &= \left(v_x^2 + v_y^2 + v_z^2\right)^{-1/2} \\ &\approx \left(\left(v_x^{(0)} + v_x^{(1)} + v_x^{(2)} + v_x^{(3)}\right)^2 \right. \\ &\quad + \left(v_y^{(0)} + v_y^{(1)} + v_y^{(2)} + v_y^{(3)}\right)^2 \\ &\quad \left. + \left(v_z^{(0)} + v_z^{(1)} + v_z^{(2)} + v_z^{(3)}\right)^2\right)^{-1/2} \\ &= \frac{1}{|v^{(0)}|}(1+T)^{-1/2}, \end{aligned} \quad \text{(A3)}$$

where

$$|v^{(0)}| = \left(\left(v_x^{(0)}\right)^2 + \left(v_y^{(0)}\right)^2 + \left(v_z^{(0)}\right)^2\right)^{1/2}, \quad \text{(A4)}$$

and

$$\begin{aligned} T = \frac{1}{|v^{(0)}|^2}&\left(2\left(v_x^{(0)}v_x^{(1)} + v_y^{(0)}v_y^{(1)} + v_z^{(0)}v_z^{(1)}\right)\right. \\ &+ \left(v_x^{(1)2} + v_y^{(1)2} + v_z^{(1)2}\right) \\ &+ 2\left(v_x^{(0)}v_x^{(2)} + v_y^{(0)}v_y^{(2)} + v_z^{(0)}v_z^{(2)}\right) \\ &+ 2\left(v_x^{(0)}v_x^{(3)} + v_y^{(0)}v_y^{(3)} + v_z^{(0)}v_z^{(3)}\right) \\ &\left. + 2\left(v_x^{(1)}v_x^{(2)} + v_y^{(1)}v_y^{(2)} + v_z^{(1)}v_z^{(2)}\right) + O\left(\sigma_Y^4\right)\right). \end{aligned} \quad \text{(A5)}$$

Applying Taylor expansion to (A3) and truncating it at the third order give

$$W \approx \frac{1}{|v^{(0)}|}\left(1 - \frac{1}{2}T + \frac{3}{8}T^2 - \frac{5}{16}T^3\right). \quad \text{(A6)}$$

Substituting (A5) in (A6) and separating W at different orders $W^{(m)}$ yield

$$W^{(0)} = \frac{1}{|v^{(0)}|}, \quad \text{(A7)}$$

$$W^{(1)} = \frac{-1}{|v^{(0)}|^3}\left(v_x^{(0)}v_x^{(1)} + v_y^{(0)}v_y^{(1)} + v_z^{(0)}v_z^{(1)}\right), \quad \text{(A8)}$$

$$\begin{aligned} W^{(2)} = \frac{-1}{2|v^{(0)}|^3}&\left(v_x^{(1)2} + v_y^{(1)2} + v_z^{(1)2} + 2v_x^{(0)}v_x^{(2)}\right. \\ &\left. + 2v_y^{(0)}v_y^{(2)} + 2v_z^{(0)}v_z^{(2)}\right) + \frac{3}{2|v^{(0)}|^5} \\ &\cdot \left(v_x^{(0)}v_x^{(1)} + v_y^{(0)}v_y^{(1)} + v_z^{(0)}v_z^{(1)}\right)^2, \end{aligned} \quad \text{(A9)}$$

$$\begin{aligned} W^{(3)} = \frac{-1}{|v^{(0)}|^3}&\left(v_x^{(0)}v_x^{(3)} + v_y^{(0)}v_y^{(3)} + v_z^{(0)}v_z^{(3)}\right. \\ &\left. + v_x^{(1)}v_x^{(2)} + v_y^{(1)}v_y^{(2)} + v_z^{(1)}v_z^{(2)}\right) \\ &+ \frac{3}{2|v^{(0)}|^5}\left(v_x^{(0)}v_x^{(1)} + v_y^{(0)}v_y^{(1)} + v_z^{(0)}v_z^{(1)}\right) \\ &\cdot \left(v_x^{(1)2} + v_y^{(1)2} + v_z^{(1)2} + 2v_x^{(0)}v_x^{(2)} + 2v_y^{(0)}v_y^{(2)} + 2v_z^{(0)}v_z^{(2)}\right) \\ &- \frac{5}{2|v^{(0)}|^7}\left(v_x^{(0)}v_x^{(1)} + v_y^{(0)}v_y^{(1)} + v_z^{(0)}v_z^{(1)}\right)^3. \end{aligned} \quad \text{(A10)}$$

Up to third order in σ_Y, U_x can be approximated as

$$U_x \approx \left(v_x^{(0)} + v_x^{(1)} + v_x^{(2)} + v_x^{(3)}\right)^2. \quad \text{(A11)}$$

Separating U_x at different orders gives

$$U_x^{(0)} = \left(v_x^{(0)}\right)^2, \quad \text{(A12)}$$

$$U_x^{(1)} = 2v_x^{(0)}v_x^{(1)}, \quad \text{(A13)}$$

$$U_x^{(2)} = 2v_x^{(0)}v_x^{(2)} + \left(v_x^{(1)}\right)^2, \quad \text{(A14)}$$

$$U_x^{(3)} = 2v_x^{(0)}v_x^{(3)} + 2v_x^{(1)}v_x^{(2)}. \quad \text{(A15)}$$

D_{xxL} can be approximated as

$$\begin{aligned} D_{xxL} &= \alpha_L U_x W \\ &\approx \alpha_L\left(U_x^{(0)} + U_x^{(1)} + U_x^{(2)} + U_x^{(3)}\right) \\ &\quad \cdot \left(W^{(0)} + W^{(1)} + W^{(2)} + W^{(3)}\right). \end{aligned} \quad \text{(A16)}$$

Separating D_{xxL} at different orders gives

$$D_{xxL}^{(0)} = \alpha_L U_x^{(0)} W^{(0)}, \tag{A17}$$

$$D_{xxL}^{(1)} = \alpha_L \left(U_x^{(0)} W^{(1)} + U_x^{(1)} W^{(0)} \right), \tag{A18}$$

$$D_{xxL}^{(2)} = \alpha_L \left(U_x^{(0)} W^{(2)} + U_x^{(1)} W^{(1)} + U_x^{(2)} W^{(0)} \right), \tag{A19}$$

$$D_{xxL}^{(3)} = \alpha_L \left(U_x^{(0)} W^{(3)} + U_x^{(1)} W^{(2)} + U_x^{(2)} W^{(1)} + U_x^{(3)} W^{(0)} \right). \tag{A20}$$

Similarly one can formulate the expansions of D_{xxTH} and D_{xxTV} at different orders. D_{xx} (equation A2) can then be approximated up to the third order in σ_Y as

$$D_{xx} \approx D_{xx}^{(0)} + D_{xx}^{(1)} + D_{xx}^{(2)} + D_{xx}^{(3)}, \tag{A21}$$

where

$$D_{xx}^{(0)} = D_{xxL}^{(0)} + D_{xxTH}^{(0)} + D_{xxTV}^{(0)} + D^*, \tag{A22}$$

$$D_{xx}^{(1)} = D_{xxL}^{(1)} + D_{xxTH}^{(1)} + D_{xxTV}^{(1)}, \tag{A23}$$

$$D_{xx}^{(2)} = D_{xxL}^{(2)} + D_{xxTH}^{(2)} + D_{xxTV}^{(2)}, \tag{A24}$$

$$D_{xx}^{(3)} = D_{xxL}^{(3)} + D_{xxTH}^{(3)} + D_{xxTV}^{(3)}. \tag{25}$$

Because of the identical structure as shown in (2), the above procedure applies exactly to the derivations of D_{yy} and D_{zz} and will be not repeated here.

[46] To derive the expansions for the cross terms $D_{xy} = D_{yx} = (\alpha_L - \alpha_{TH}) v_x v_y / |v|$, letting $R_{xy} = v_x v_y$ and substituting in the velocity expansions up to the third order, and then separating it at different orders, one obtains

$$R_{xy}^{(0)} = v_x^{(0)} v_y^{(0)}, \tag{A26}$$

$$R_{xy}^{(1)} = v_x^{(0)} v_y^{(1)} + v_x^{(1)} v_y^{(0)}, \tag{A27}$$

$$R_{xy}^{(2)} = v_x^{(0)} v_y^{(2)} + v_x^{(1)} v_y^{(1)} + v_x^{(2)} v_y^{(0)}, \tag{A28}$$

$$R_{xy}^{(3)} = v_x^{(0)} v_y^{(3)} + v_x^{(1)} v_y^{(2)} + v_x^{(2)} v_y^{(1)} + v_x^{(3)} v_y^{(0)}. \tag{A29}$$

$D_{xy} = D_{yx}$ can then be approximated up to the third order in σ_Y as

$$D_{xy} = D_{yx} \approx D_{xy}^{(0)} + D_{xy}^{(1)} + D_{xy}^{(2)} + D_{xy}^{(3)}, \tag{A30}$$

where

$$D_{xy}^{(0)} = D_{yx}^{(0)} = (\alpha_L - \alpha_{TH}) R_{xy}^{(0)} W^{(0)}, \tag{A31}$$

$$D_{xy}^{(1)} = D_{yx}^{(1)} = (\alpha_L - \alpha_{TH}) \left(R_{xy}^{(0)} W^{(1)} + R_{xy}^{(1)} W^{(0)} \right), \tag{A32}$$

$$D_{xy}^{(2)} = D_{yx}^{(2)} = (\alpha_L - \alpha_{TH}) \cdot \left(R_{xy}^{(0)} W^{(2)} + R_{xy}^{(1)} W^{(1)} + R_{xy}^{(2)} W^{(0)} \right), \tag{A33}$$

$$D_{xy}^{(3)} = D_{yx}^{(3)} = (\alpha_L - \alpha_{TH}) \cdot \left(R_{xy}^{(0)} W^{(3)} + R_{xy}^{(1)} W^{(2)} + R_{xy}^{(2)} W^{(1)} + R_{xy}^{(3)} W^{(0)} \right). \tag{A34}$$

The derivations of $D_{xz} = D_{zx}$ and $D_{yz} = D_{zy}$ are similar and thus not repeated here. The expansion mode coefficients for the entire dispersion tensor $D_{i_1,i_2,\ldots,i_m}^{(m)}$ can be obtained by directly substituting in the respective velocity expansion coefficients $v_{i_1,i_2,\ldots,i_m}^{(m)}$ [*Lu and Zhang*, 2004].

Appendix B: Derivations of Higher-Order Equations

[47] Separating (4) at the second and third orders, one obtains the following equations for the concentration expansions $C^{(2)}$ and $C^{(3)}$:

$$\frac{\partial C^{(2)}}{\partial t} = \nabla \cdot \left(D^{(0)} \nabla C^{(2)} \right) - \nabla \cdot \left(v^{(0)} C^{(2)} \right) + g^{(2)}, \tag{B1}$$

$$\frac{\partial C^{(3)}}{\partial t} = \nabla \cdot \left(D^{(0)} \nabla C^{(3)} \right) - \nabla \cdot \left(v^{(0)} C^{(3)} \right) + g^{(3)}, \tag{B2}$$

where

$$g^{(2)} = \nabla \cdot \left(D^{(2)} \nabla C^{(0)} + D^{(1)} \nabla C^{(1)} - v^{(2)} C^{(0)} - v^{(1)} C^{(1)} \right), \tag{B3}$$

$$g^{(3)} = \nabla \cdot \left(D^{(3)} \nabla C^{(0)} + D^{(2)} \nabla C^{(1)} + D^{(1)} \nabla C^{(2)} - v^{(3)} C^{(0)} - v^{(2)} C^{(1)} - v^{(1)} C^{(2)} \right). \tag{B4}$$

In general, at mth order, $m \geq 1$:

$$\frac{\partial C^{(m)}}{\partial t} = \nabla \cdot \left(D^{(0)} \nabla C^{(m)} \right) - \nabla \cdot \left(v^{(0)} C^{(m)} \right) + g^{(m)}, \tag{B5}$$

subject to initial and boundary conditions

$$C^{(m)}(\boldsymbol{x}, 0) = 0, \qquad \boldsymbol{x} \in \Omega, \tag{B6}$$

$$C^{(m)}(\boldsymbol{x}, t) = 0, \qquad \boldsymbol{x} \in \Gamma_D, \tag{B7}$$

$$D^{(0)}\nabla C^{(m)}\cdot\boldsymbol{n}(\boldsymbol{x}) = -\sum_{i=0}^{m-1} D^{(m-i)}\nabla C^{(i)}\cdot\boldsymbol{n}(\boldsymbol{x}), \qquad \boldsymbol{x}\in\Gamma_N, \quad \text{(B8)}$$

where

$$g^{(m)} = \nabla\cdot\sum_{i=0}^{m-1}\left(D^{(m-i)}\nabla C^{(i)} - v^{(m-i)}C^{(i)}\right). \quad \text{(B9)}$$

The governing equations for the second-and third-order mode expansion coefficients $C^{(2)}_{i_1,i_2}$ and $C^{(3)}_{i_1,i_2,i_3}$ are

$$\frac{\partial C^{(2)}_{i_1,i_2}}{\partial t} = \nabla\cdot\left(D^{(0)}\nabla C^{(2)}_{i_1,i_2}\right) - \nabla\cdot\left(v^{(0)}C^{(2)}_{i_1,i_2}\right) + g^{(2)}_{i_1,i_2}, \quad \text{(B10)}$$

$$\frac{\partial C^{(3)}_{i_1,i_2,i_3}}{\partial t} = \nabla\cdot\left(D^{(0)}\nabla C^{(3)}_{i_1,i_2,i_3}\right) - \nabla\cdot\left(v^{(0)}C^{(3)}_{i_1,i_2,i_3}\right) + g^{(3)}_{i_1,i_2,i_3}, \quad \text{(B11)}$$

where

$$g^{(2)}_{i_1,i_2} = \nabla\cdot\Big(D^{(2)}_{i_1,i_2}\nabla C^{(0)} + \left(D^{(1)}_{i_1}\nabla C^{(1)}_{i_2} + D^{(1)}_{i_2}\nabla C^{(1)}_{i_1}\right)/2 - v^{(2)}_{i_1,i_2}C^{(0)} - \left(v^{(1)}_{i_1}C^{(1)}_{i_2} + v^{(1)}_{i_2}C^{(1)}_{i_1}\right)/2\Big) \quad \text{(B12)}$$

$$\begin{aligned} g^{(3)}_{i_1,i_2,i_2} = \nabla\cdot\Big(&D^{(3)}_{i_1,i_2,i_3}\nabla C^{(0)} \\ &+ \left(D^{(2)}_{i_1,i_2}\nabla C^{(1)}_{i_3} + D^{(2)}_{i_1,i_3}\nabla C^{(1)}_{i_2} + D^{(2)}_{i_2,i_3}\nabla C^{(1)}_{i_1}\right)/3 \\ &+ \left(D^{(1)}_{i_1}\nabla C^{(2)}_{i_2,i_3} + D^{(1)}_{i_2}\nabla C^{(2)}_{i_1,i_3} + D^{(1)}_{i_3}\nabla C^{(2)}_{i_1,i_2}\right)/3 \\ &- v^{(3)}_{i_1,i_2,i_3}C^{(0)} - \left(v^{(2)}_{i_1,i_2}C^{(1)}_{i_3} + v^{(2)}_{i_1,i_3}C^{(1)}_{i_2} + v^{(2)}_{i_2,i_3}C^{(1)}_{i_1}\right)/3 \\ &- \left(v^{(1)}_{i_1}C^{(2)}_{i_2,i_3} + v^{(1)}_{i_2}C^{(2)}_{i_1,i_3} + v^{(1)}_{i_3}C^{(2)}_{i_1,i_2}\right)/3\Big). \end{aligned} \quad \text{(B13)}$$

In general, at mth order and mode $i_1,i_2,\ldots,i_m$, $m \geq 1$:

$$\frac{\partial C^{(m)}_{i_1,i_2,\ldots,i_m}}{\partial t} = \nabla\cdot\left(D^{(0)}\nabla C^{(m)}_{i_1,i_2,\ldots,i_m}\right) - \nabla\cdot\left(v^{(0)}C^{(m)}_{i_1,i_2,\ldots,i_m}\right) + g^{(m)}_{i_1,i_2,\ldots,i_m}, \quad \text{(B14)}$$

subject to initial and boundary conditions

$$C^{(m)}_{i_1,i_2,\ldots,i_m}(\boldsymbol{x},0) = 0, \qquad \boldsymbol{x}\in\Omega, \quad \text{(B15)}$$

$$C^{(m)}_{i_1,i_2,\ldots,i_m}(\boldsymbol{x},t) = 0, \qquad \boldsymbol{x}\in\Gamma_D, \quad \text{(B16)}$$

$$D^{(0)}\nabla C^{(m)}_{i_1,i_2,\ldots,i_m}\cdot\boldsymbol{n}(\boldsymbol{x}) = -\sum_{k=0}^{m-1}\left[\frac{(m-k)!}{m!}\cdot\sum_{P_{i_1,i_2,\ldots,i_m}}\left(D^{(m-k)}_{i_{k+1},\ldots,i_m}\nabla C^{(k)}_{i_1,\ldots,i_k}\right)\right]\cdot\boldsymbol{n}(\boldsymbol{x}), \quad \boldsymbol{x}\in\Gamma_N, \quad \text{(B17)}$$

where

$$g^{(m)}_{i_1,i_2,\ldots,i_m} = \nabla\cdot\sum_{k=0}^{m-1}\left[\frac{(m-k)!}{m!}\cdot\sum_{P_{i_1,i_2,\ldots,i_m}}\left(D^{(m-k)}_{i_{k+1},\ldots,i_m}\nabla C^{(k)}_{i_1,\ldots,i_k} - v^{(m-k)}_{i_{k+1},\ldots,i_m}C^{(k)}_{i_1,\ldots,i_k}\right)\right]. \quad \text{(B18)}$$

The summation $\sum_{P_{i_1,i_2,\ldots,i_m}}$ in (B17) and (B18) is taken over a subset of the permutation of $\{i_1, i_2,\ldots, i_m\}$ in which repeated terms of $D^{(m-k)}_{i_{k+1},\ldots,i_m}\nabla C^{(k)}_{i_1,\ldots,i_k}$ and $v^{(m-k)}_{i_{k+1},\ldots,i_m}C^{(k)}_{i_1,\ldots,i_k}$ are excluded. For example, $\sum_{P_{i_1,i_2,i_3}} D^{(1)}_{i_1}\nabla C^{(2)}_{i_2,i_3} = D^{(1)}_{i_1}\nabla C^{(2)}_{i_2,i_3} + D^{(1)}_{i_2}\nabla C^{(2)}_{i_1,i_3} + D^{(1)}_{i_3}\nabla C^{(2)}_{i_1,i_2}$. $D^{(1)}_{i_1}\nabla C^{(2)}_{i_3,i_2}$ is identical to $D^{(1)}_{i_1}\nabla C^{(2)}_{i_2,i_3}$ and thereby excluded as $C^{(2)}_{i_2,i_3}$ calculated this way is symmetric with respect to its subscript indices. Furthermore, because of the symmetry, we only need to solve $C^{(m)}_{i_1,i_2,\ldots,i_m}$ for $i_1 \leq i_2 \leq \cdots \leq i_m$ as $C^{(m)}_{i_1,i_2,\ldots,i_m}$ for $i_1 > i_2 > \cdots > i_m$ can be directly obtained by simple manipulation of the subscripts.

[48] **Acknowledgments.** This work is partially supported by the U.S. National Science Foundation through grant OISE0511496, by the American Chemical Society through its Petroleum Research Fund (grant 42109-AC9), and by the National Natural Science Foundation of China through grants 50310444 and 50688901.

References

Burnett, R. D., and E. O. Frind (1987), An alternating direction Galerkin technique for simulation of groundwater contaminant transport in three dimensions: 2 Dimensionality effects, *Water Resour. Res.*, *23*, 695–705.

Chen, M., D. Zhang, A. A. Keller, and Z. Lu (2005), A stochastic analysis of steady state two-phase flow in heterogeneous media, *Water Resour. Res.*, *41*, W01006, doi:10.1029/2004WR003412.

Cushman, J. H. (1997), *The Physics of Fluids in Hierarchical Porous Media: Angstroms to Miles*, Kluwer Acad., Norwell, Mass.

Dagan, G. (1984), Solute transport in heterogeneous formations, *J. Fluid Mech.*, *145*, 151–177.

Dagan, G. (1989), *Flow and Transport in Porous Formations*, Springer, New York.

Dagan, G., and A. Fiori (1997), The influence of pore-scale dispersion on concentration statistical moments in transport through heterogeneous aquifers, *Water Resour. Res.*, *33*, 1595–1605.

Dagan, G., V. Cvetkovic, and A. Shapiro (1992), A solute flux approach to transport in heterogeneous formations: 1. The general framework, *Water Resour. Res.*, *28*, 1369–1376.

Darvini, G., and P. Salandin (2006), Nonstationary flow and nonergodic transport in random porous media, *Water Resour. Res.*, *42*, W12409, doi:10.1029/2005WR004846.

Gelhar, L. W. (1993), *Stochastic Subsurface Hydrology*, Prentice-Hall, Englewood Cliffs, N. J.

Gelhar, L. W., A. L. Gutiahr, and R. L. Naff (1979), Stochastic analysis of macrodispersion in a stratified aquifer, *Water Resour. Res.*, *15*, 1387–1397.

Ghanem, R., and S. Dham (1998), Stochastic finite element analysis for multiphase flow in heterogeneous porous media, *Transp. Porous Media*, *32*, 239–262.

Ghanem, R., and D. Spanos (1991), *Stochastic Finite Elements: A Spectral Approach*, Springer, New York.

Graham, W. D., and D. McLaughlin (1989), Stochastic analysis of nonstationary subsurface solute transport: 1. Unconditional moments, *Water Resour. Res.*, *25*, 215–232.

Harbaugh, A. W., E. R. Banta, M. C. Hill, and M. G. McDonald (2000), MODFLOW-2000, the U.S. Geological Survey modular ground-water model—User guide to modularization concepts and the ground-water flow processes, *U.S. Geol. Surv. Open File Rep., 00–92*, 121 pp.

Hassan, A. E., J. H. Cushman, and J. W. Delleur (1998), A Monte Carlo assessment of Eulerian flow and transport perturbation models, *Water Resour. Res.*, *34*, 1143–1163.

Hu, B. X., A. E. Hassan, and J. H. Cushman (1999), Eulerian solutions of $O(\sigma_v^N)$ for the stochastic transport problem for conservative tracers coupled with $O(\sigma_f^4)$ solutions for the flow problem in an infinite domain, *Water Resour. Res.*, *35*, 3685–3697.

Kapoor, V., and L. W. Gelhar (1994a), Transport in three-dimensional heterogeneous aquifers: 1. Dynamics of concentration fluctuations, *Water Resour. Res.*, *30*, 1775–1788.

Kapoor, V., and L. W. Gelhar (1994b), Transport in three-dimensional heterogeneous aquifers: 2. Predictions and observations of concentration fluctuations, *Water Resour. Res.*, *30*, 1789–1801.

Kapoor, V., and P. K. Kitanidis (1997), Advection-diffusion in spatially random flows: Formulation of concentration covariance, *Stochastic Hydrol. Hydraul.*, *11*, 397–422.

Liu, G., D. Zhang, and Z. Lu (2006), Stochastic uncertainty analysis for unconfined flow systems, *Water Resour. Res.*, *42*, W09412, doi:10.1029/2005WR004766.

Lu, Z., and D. Zhang (2004), Conditional simulations of flow in randomly heterogeneous porous media using a KL-based moment-equation approach, *Adv. Water Resour.*, *27*, 859–874.

Morales-Casique, E., S. P. Neuman, and A. Guadagnini (2006a), Non-local and localized analyses of non-reactive solute transport in bounded randomly heterogeneous porous media: Theoretical framework, *Adv. Water Resour.*, *29*(8), 1238–1255.

Morales-Casique, E., S. P. Neuman, and A. Guadagnini (2006b), Nonlocal and localized analyses of nonreactive solute transport in bounded randomly heterogeneous porous media: Computational analysis, *Adv. Water Resour.*, *29*(9), 1399–1418.

Neuman, S. P. (1993), Eulerian-Lagrangian theory of transport in space-time nonstationary velocity fields: Exact nonlocal formalism by conditional moments and weak approximations, *Water Resour. Res.*, *29*, 633–645.

Neuman, S. P. (2006), Blueprint for perturbative solution of flow and transport in strongly heterogeneous composite media using fractal and variational multiscale decomposition, *Water Resour. Res.*, *42*, W06D04, doi:10.1029/2005WR004315.

Neuman, S. P., and Y. K. Zhang (1990), A quasi-linear theory of non-Fickian and Fickian subsurface dispersion: 1. Theoretical analysis with application to isotropic media, *Water Resour. Res.*, *26*, 887–902.

Rubin, Y. (2003), *Applied Stochastic Hydrogeology*, Oxford Univ. Press, Oxford, U. K.

Salandin, P., and V. Fiorotto (2000), Dispersion tensor evaluation in heterogeneous media for finite Peclet values, *Water Resour. Res.*, *36*, 1449–1455.

Yang, J., D. Zhang, and Z. Lu (2004), Stochastic analysis of saturated-unsaturated flow in heterogeneous media by combining Karhunen-Loève expansion and perturbation method, *J. Hydrol.*, *294*, 18–38.

Zhang, D. (2002), *Stochastic Methods for Flow in Porous Media: Coping With Uncertainties*, 350 pp., Elsevier, New York.

Zhang, D., and Z. Lu (2004), An efficient, high-order perturbation approach for flow in random porous media via Karhunen–Loève and polynomial expansions, *J. Comput. Phys.*, *194*, 773–794.

Zhang, D., and S. P. Neuman (1995), Eulerian-Lagrangian analysis of transport conditioned on hydraulic data: 1. Analytical-numerical approach, *Water Resour. Res.*, *31*, 39–51.

Zhang, D., and S. P. Neuman (1996), Effect of local dispersion on solute transport in randomly heterogeneous media, *Water Resour. Res.*, *32*, 2715–2723.

Zheng, C., and P. P. Wang (1999), MT3DMS: A modular three-dimensional multispecies model for simulation of advection, dispersion and chemical reactions of contaminants in groundwater systems; documentation and user's guide, *Contract Rep. SERDP-99-1*, U.S. Army Eng. Res. and Dev. Cent., Vicksburg, Miss.

G. Liu, Kansas Geological Survey, University of Kansas, 1930 Constant Avenue, Lawrence, KS 66047, USA. (gliu@kgs.ku.edu)

Z. Lu, Hydrology and Geochemistry Group, Los Alamos National Laboratory, Los Alamos, NM 87545, USA.

D. Zhang, Department of Civil and Environmental Engineering and Mork Family Department of Chemical Engineering and Material Sciences, University of Southern California, Los Angeles, CA 90089, USA.